Lab on a Chip

Accepted Manuscript

ROYAL SOCIETY OF CHEMISTRY

www.rsc.org/loc

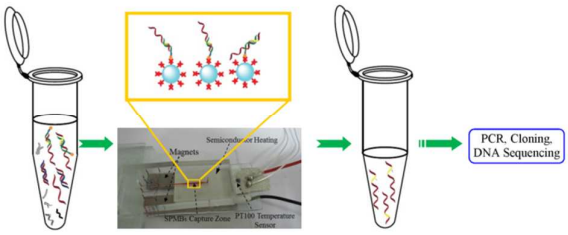

We present a novel magnetic system in microfluidic channels for fast and effective isolation of simple sequence repeat markers.

Journal Name

RSCPublishing

ARTICLE

Fast Magnetic Isolation of Simple Sequence Repeat Markers in Microfluidic Channels†

Cite this: DOI: 10.1039/xoxxoooooox

Shibin He [a, b, 1], Xu Yu [a, 1], Xiangwu Wang [b], Junjun Tan [a], Shihan Yan [a], Pu Wang [a], Bi-Hai Huang [a], Zhi-Ling Zhang [a *], Lijia Li [a *]

Received ooth January 2012,
Accepted ooth January 2012

DOI: 10.1039/xoxxoooooox

www.rsc.org/

Simple sequence repeat (SSR) markers are widely used for genome mapping, genetic diversity characterization and medical diagnosis. The fast isolation by AFLP of sequence containing repeats (FIASCO) is a powerful method for SSR marker isolation, but it is laborious, costly, and time consuming and requires multiple rounds of washing. Here, we report a superparamagnetic bead (SPMB)-based FIASCO method in a magnetic field controllable microfluidic chip (MFCM-Chip). This method dramatically reduces the assay time by 4.25-fold and reduces the quantity of magnetic beads and probes by 10-fold through the magnetic capture of (AG)n-containing fragments from Herba Leonuri, followed by washing and eluting on a microchip. The feasibility of this method was further evaluated by PCR and sequencing, and the results showed that the proportion of fragments containing SSRs was 89%, confirming that this platform is a fast and efficient method for SSR marker isolation. This cost-effective platform will make the powerful FIASCO technique more accessible for routine use with a wide variety of materials.

Introduction

Various types of molecular markers have been developed, including simple sequence repeats (SSRs), amplified fragment length polymorphisms (AFLPs), and randomly amplified polymorphic DNAs (RAPDs) [1]. The use of these molecular markers has contributed significantly to gene mapping, genetic variation assays, and medical diagnostics [2-4]. SSRs, which are also known as microsatellites, usually comprise a sequence of 2, 3, or 4 nucleotides that is repeated 3 to 100 times. The use of SSRs has become increasingly popular because of their high polymorphism and abundance in the genome, high reproducibility and easy data scoring and co-dominance [5, 6]. However, unlike AFLPs, RAPDs and other markers, SSR markers are species specific and must be isolated *de novo* from the species analyzed for the first time [7].

Fast isolation by AFLP of sequence containing repeats (FIASCO) is a widely used tool for SSR marker isolation [7]. In a conventional FIASCO procedure, SSR-containing fragments are selectively hybridized to biotinylated microsatellite probes and captured by streptavidin-magnetic beads. The DNA-probe-bead complexes are then separated from the hybridization mixture by a magnetic field, and the nonspecifically bound DNAs are removed by multiple rounds of washing. It consumes a large number of reagents and involves complex and tedious manual processes such as mixing, tube-transfer, and pipetting in an Eppendorf tube during the pivotal magnetic bead-based selection step. The long manual wash time tends to cause substantial material loss, and inefficient washing results in a large proportion of nonspecific DNA. Substantial operator experience and careful manipulation of a small amount of target DNA and magnetic beads are required.

Microfluidic technology can integrate multiple laboratory functions on a small, closed chip, enabling the manipulation of extremely small amounts of liquids and particles [8]. A number of novel physical phenomena that occur on the microscale can make highly pure molecule separation and highly sensitive detection within a dramatically shorter period of time. In addition, this method has the advantages of automation, and lower reagent consumption and cost [9]. Recently, microfluidic technology has been extensively explored to automate miniature devices and systems for biological and medical analyses, including fluorescence in situ hybridization (FISH) mapping, chromatin immunoprecipitation (ChIP), and aptamer selection [10-13]. Magnetic beads are easy to manipulate and functionalize, and are widely used in many fields. Combining microfluidic chip technology with magnetic beads has many advantages compared with the traditional magnetic bead-based method in an Eppendorf tube [14-16]. Gijset al. used two magnets to trap the magnetic nanoparticles to form the chains for immunoassay and could detect antibodies with very low concentrations [17]. Three pairs of magnets were used to trap different antibody modified magnetic beads and generate three plugs for simultaneous detection of several proteins [18]. Viovy et al. used the magnetic bead plugs for protein digestion and obtained high digestion efficiency [19].

Integrating microfluidic chip technology with a magnetic bead-based FIASCO procedure might represent an improvement over the Eppendorf tube method. However, efficient control of the magnetic bead in a microfluidic chip at high flow velocity is a prerequisite for magnetic bead-based applications. We previously developed a device in which superparamagnetic beads (SPMBs) could be captured at high velocity for bioanalysis [20, 21]. In this study, we proposed an SPMB-based FIASCO method in a magnetic field-controllable microfluidic chip (MFCM-Chip). As a proof-of-concept, this device was used to separate $(AG)_n$-containing fragments from Herba Leonuri. The MFCM-Chip decreased the quantity of magnetic beads and probes by 10-fold and decreased the labour time by 4.25-fold. Subsequent PCR and sequencing analysis demonstrated that the proportion of SSR-containing fragments was 89%, confirming that this method is fast and efficient for SSR marker isolation. The MFCM-Chip could be reused repeatedly only by a simple ultrasonic washing process. This device takes advantage of the unique

phenomena of microscale reactions, and we believe this cost-effective platform will make the powerful FIASCO technique more accessible for routine use with a wide variety of materials.

Experimental Section

The entire procedure is illustrated in Figure 1, and the methods for preparing streptavidin-coated superparamagnetic beads and DNA-probe complexes, designing and fabricating the MFCM-Chip, and sequencing and analysing the SSR are included in the Electronic Supplementary Information (ESI). The whole MFCM-Chip was assembled using valve control channels, fluidic channels, a nickel pattern, two permanent magnets, semiconductor heating, and a PT100 temperature sensor (Fig. 1 and Fig. S1). The two permanent magnets provided the external magnetic field, and the nickel pattern was able to generate high magnetic field gradients for SPMB capture. The denaturation efficiency of the FIASCO method is strongly affected by temperature, and thus, the temperature in the channel must be calibrated. As shown in Figure 1, the temperature calibration was controlled by a homemade temperature testing system in which a semiconductor was used for heat and the temperature was detected by a PT100 temperature sensor.

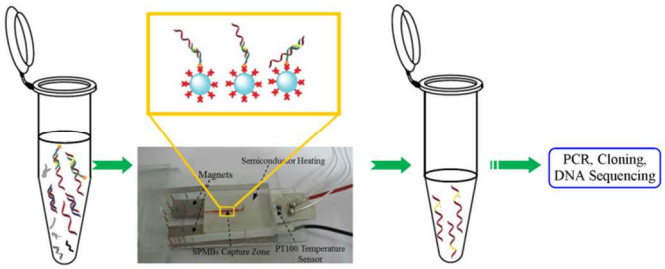

Fig.1 A schematic illustration of the entire magnetic isolation procedure for SSR markers.

Results and discussion

Overview of the SPMB-based FIASCO method in an MFCM-Chip

In this study, we proposed an SPMB-based FIASCO method in an MFCM-Chip to separate $(AG)_n$-containing fragments from Herba Leonuri (Fig. S2). The isolation assay began with the preparation of DNA-probe hybrids (Fig. S2a) and SA-SPMBs (Fig. S3a). Herba Leonuri genomic DNA was digested with the restriction enzyme *Mse*I, and fragments ranging from 200 to 800 bp were ligated to adaptors (*Mse*I A and *Mse*I B). The ligation mixture was then amplified with the specific primer *Mse*I-N. Microsatellite-containing fragments were selectively hybridized to biotinylated microsatellite probes. The synthesized SA-SPMBs and DNA-probe hybrids were separately loaded into the MFCM-Chip (Fig. S2b). The microsatellite-containing fragments were separated after incubation, washing, and denaturation. The entire magnetic separation process in the MFCM-Chip required about 20 min. Finally, the fragments were cloned and sequenced to obtain SSR markers (Fig. S2c).

Characterization of SA-SPMBs by DLS

SPMBs have been widely applied to isolate biological materials, particularly in miniaturized and automated settings, because of their small size, easy manipulation by magnets, and their ability to be functionalized by ligands or biomolecules such as antibodies, streptavidin (SA), DNA/RNA, or other molecules [14-16]. When SPMBs are coupled with SA, they offer an efficient means of isolating biotinylated molecules [22, 23]. In this study, SPMBs with carboxyl groups were conjugated with SA (Fig. S3a). The average hydrodynamic diameter of the SPMBs was approximately 526.4 ± 15.4 nm, with a PDI (polydispersity index) of 0.063, suggesting that the SPMBs were monodispersed with fairly uniform sizes (Fig. S3b). The mean hydrodynamic diameter of the SA-SPMBs was 719.5 ± 4.6 nm, with a narrow size distribution (PDI 0.051, Fig. S3b). This diameter is greater than that of the SPMBs, indicating that SA was conjugated to the SPMBs. In addition, the synthesized SA-SPMBs were smaller than commercially available SA-magnetic beads (1-2 μm) [24], potentially reducing steric hindrance and increasing binding capacity during hybridization with biotinylated probes.

Simulating the absolute value of the magnetic field gradient ($|\nabla \mathbf{B}|$)

Inducing a strong local magnetic field gradient is a prerequisite for controlling SPMB patterns in microfluidic chips at high flow velocities [25, 26]. On the basis of our previous work [20, 21], we employed a nickel pattern embedded in thin poly (dimethylsiloxane) prepolymer (PDMS) to control the magnetic field distribution in the microfluidic chip. We used COMSOL Multiphysics 4.3 to simulate the absolute value of the magnetic field gradient ($|\nabla B|$) in the area of the nickel pattern. In the simulation, the microfluidic chip was placed 3.5 mm above the two permanent magnets. The two magnets were put under each side of the microchannel (the gap between the two magnets was 6 mm) and generated an 'NS' pole (as the direction of Y-axis) magnetic field through the microchannel, which could also be seen in Figure 1. The nickel patterns were about 9 μm height, and the thin PDMS on the nickel patterns was about 1-2 μm, which did not influence the magnetic field gradients induced by nickel patterns. According to the properties of the permanent magnets, the remnant magnetic flux density (B_r) is 1.17 T, and the relative permeability (μ_r) is 1.05. The result of the simulation indicated the presence of a high magnetic field gradient ($|\nabla B|$)) at the nickel pattern units (Fig. S4a), due to the relative magnetic permeability of nickel ($\mu_{r\,(\text{nickel})} \approx 200$) is a great contrast to that of fluid ($\mu_{r\,(\text{buffer})} \approx 1$) [27]. The absolute value of the magnetic field gradient ($|\nabla B|$)) could be described by the following equation [24,25]:

$$|\nabla B| = \sqrt{\left(\frac{\partial B}{\partial x}\right)^2 + \left(\frac{\partial B}{\partial y}\right)^2}$$

The ($|\nabla B|$) was approximately 40000 ~ 50000 $T \cdot m^{-1}$ (Fig. S4b) at the nickel pattern arrays. Thus, the SA-SPMBs at this high magnetic field gradient could be captured between the two nickel pattern units as the direction of external magnetic field (Y-axis direction), even at a high velocity.

Magnetic separation of SSR-containing fragments in the MFCM-Chip

The MFCM-Chip was placed under an inverted microscope (TE2000-U, Nikon, Tokyo, Japan) to monitor the entire process. The entire procedure for separating $(AG)_n$-containing fragments from Herba Leonuri in the MFCM-Chip is illustrated in Fig. S2b and summarized in Table S1. During the magnetic separation process, we used the valve to control the sample and washing buffer loading processes. The valves were controlled by a programme written with Matlab software. After blocking the microfluidic channel with 1% BSA, we injected N_2 into valves 1, 2, 4, and 5. These valves were then closed, and valve 3 was opened (Fig. 2c(A)). About 0.1 mg SA-SPMBs were loaded into the MFCM-Chip (as shown in Fig. 2a) at a speed of 40 μL/min for 5 min with valves 1, 2, 4, and 5 closed. At this point, the redundant solution could be discharged from outlet 3 without contaminating other outlets. Figure 2c(B) shows that valves 1, 2, and 3 were all closed when N_2 was injected, and therefore the outlets could not be used. We monitored the nickel pattern area by inverted microscopy to determine if the SA-SPMBs could be

captured at the pattern. The nickel pattern in the microfluidic channel is displayed in Fig. S5a. The SA-SPMBs were captured at the nickel pattern areas at a relatively high flow velocity (Fig. S5b).

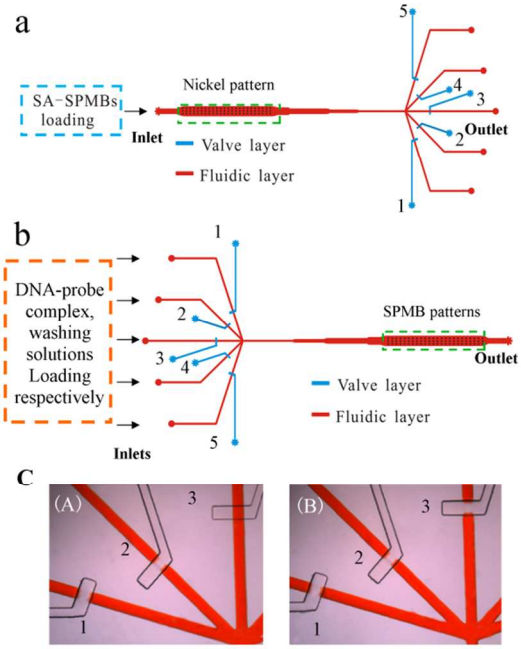

Fig.2 Sample loading and washing processes in the MFCM-Chip used to separate SSR-containing fragments. (a) The SA-SPMB loading process. (b) The loading process for the DNA-probe complex and washing solution. (c) Ink experiments showing the valve-controlled injection process. A. Valves 1 and 2 were closed, and valve 3 was open; thus the fluid was blocked at valves 1 and 2 and could only pass from inlet 3. B. Valves 1, 2, and 3 were closed, and thus the fluid was blocked at valves 1, 2, and 3 and could not pass from any inlet.

We changed the inlet and outlet after finishing the SA-SPMB loading process, as shown in Fig. S2b. Valves 1, 2, 4, and 5 remained closed, and valve 3 remained open. TEN_{100} was loaded from inlet 3 to wash the SA-SPMBs to enhance the reactivity of the SA-SPMBs with the DNA-probe complexes. The flow velocity was set to 20 μL/min, and the washing process lasted for 2 min. Valves 2, 3, 4, and 5 were then closed, and valve 1 was opened. The DNA-probe complex samples (5 μL, about 50 ng DNA and 25 nM probe) were loaded from inlet 1. DNA-probe loading was first performed at 5 μL/min for 1 min, and the DNA-probe complexes were then incubated with SA-SPMBs in the MFCM-Chip for 2 min. It was possible to capture DNA-probe complexes with SA-SPMBs during this process because of the high affinity reaction between SA and the biotinylated probes.

After the incubation, we employed different solutions to remove nonspecifically bound materials; these materials were more efficiently removed by fast continuous washing in microfluidic channels compared to the traditional pipetting method in an Eppendorf tube. Valves 1, 3, 4, and 5 were closed, and valve 2 was opened. The TEN_{1000} solution was loaded from inlet 2. The whole microchannel was washed with TEN_{1000} at 20 μL/min, and this process lasted for 2 min. Valves 1, 2, 3, and 5 were then closed, and valve 4 was opened. A 0.2×SSC solution containing 0.1% SDS was injected from inlet 4 at 20 μL/min for 2 min, and this stringent washing process removed nonspecific binding materials more effectively. Actually most of DNAs would be washed off because the genome only contains a very low proportion of (AG)n repeats, although we did not know exactly (AG)n contents in this genome.

Finally, valves 1, 2, 3, and 4 were closed, and valve 5 was opened. The TE buffer was loaded from inlet 5, and the whole microchannel was washed with TE buffer. The TE buffer was collected from the outlet before denaturation as a negative control for the subsequent PCR experiment. The separation efficiency of SSR-containing fragments is strongly affected by temperature. Therefore, it was necessary to precisely control the chamber temperature. We used a homemade semiconductor heating and temperature control device to maintain the temperature at 95 ℃ for DNA denaturation as shown in Fig. 1. To fully denature the DNA, the loading speed of the TE buffer was slowed to 5 μL/min for 5min. We collected the TE buffer containing the DNA sample at 95 ℃. The entire magnetic separation process in the MFCM-Chip could be completed within 20 min. When compared with the conventional method, this assay provided an approximately 4.25-fold reduction in time and a 10-fold reduction in SPMBs and probes; an even greater reduction in washing solution volume was also observed (Table S1).

Specificity and sensitivity of the magnetic isolation of the SSR marker in the MFCM-Chip

To determine the specificity of the magnetic isolation of the SSR markers in the MFCM-Chip, the TE buffers collected before and after denaturation were precipitated with ethanol and resuspended in ddH_2O, respectively, for use as the PCR templates. If the biotinylated DNAs were tightly bound to the SA-SPMBs and the nonspecific DNAs were completely removed during the washing process, PCR products should not be obtained when the TE buffer collected before denaturation was used as the template. As expected, the TE buffer collected before denaturation did not yield any amplified DNA bands when used as the template (Lane 2, Fig. 3a), while bands ranging from 200 to 800 bp were observed when the TE buffer collected after denaturation was used as the template (Lane 1, Fig. 3a). The concentration of DNA marker was 10 ng/μL, and we loaded 2 μL DNA marker in a gel electrophoresis experiment, so the DNA content was about 20 ng in the marker lane (Fig. 3a). Analysis of the brightness of the PCR product bands visualized in Fig. 3a (Lane 1) using Quantity One 1-D analysis software showed that the yield of PCR was about 100 ng (2.5 μL). Therefore, as the total volume of PCR products was 25 μL, the amount of the recovered DNA fragments after PCR amplification was about 1000 ng. In the traditional FIASCO method, the starting DNAs are about 1000 ng in order to get such amount of DNAs after PCR (data not shown). These results demonstrated that the nonspecific DNAs were completely removed during the washing process and that no free DNA was present in the MFCM-Chip.

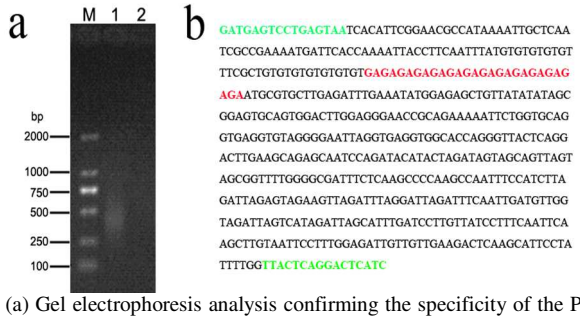

Fig.3 (a) Gel electrophoresis analysis confirming the specificity of the PCR-recovered fragments. Lane M: DNA marker (DL 2000); lane 1: PCR-amplification of specific recovered fragments from the TE solution collected after denaturation at 95 °C for 5 min; lane 2: negative control (in which the TE solution collected before denaturation was used as the template for PCR). (b) The sequence of the clone containing SSRs. The SSR sequences are red, and the forward and inverted primer sequences are green.

To determine if the separated fragments from the MFCM-Chip contained any SSRs, we cloned and sequenced these fragments and analyzed their sequences with an SSR finder tool. Because biotin-T_{10}-$(AG)_{13}$ was used as a probe in this study, we simply counted the

repeating AG, GA, TC, or CT units in the sequences. The repeat was only designated an SSR locus when the number of repeats in the clone sequence was greater than or equal to three of a clone [6]. An SSR locus may be designed as an SSR marker. We sequenced 27 DNA fragments, and 24 contained repeating units of AG, GA, TC, or CT. Thus, the proportion of positive clones was 89%. These results are summarized in Table S2. The positive clones are arrayed from 1-24 in the vertical column, and the numbers in the horizontal column represent the number of repeats (Table S2). The frequency of the number of repeats was counted in every positive clone (Table S2). From Table S2, the number of repeats in the 24 clones was all greater than or equal to three; some clones contained 1 locus of repeat units, and others contained several loci of repeat units. The several loci of repeat units in a clone may be designed as several SSR markers. For example, clone No.14 (Table S2) had 2 loci with repeat units; one was repeated 6 times, while the other was repeated 7 times. Therefore, the two loci with repeat units in this clone may be designed as two SSR markers.

Removing nonspecific DNAs by pipetting in the traditional method usually and easily damages the DNA fragments, making them unusable for designing oligonucleotide primers on both sides of the SSRs. By controlling the flow rate in the MFCM-Chip, the DNA sample was not damaged. The sequence of a representative clone (clone No.20, Table S2) is shown in Fig. 3b; the whole sequence was intact. The flanking sequences between the SSRs can be used to design oligonucleotide primers. If the oligonucleotide primers could amplify fragments of different lengths in different species, they could be used as markers to further assay genetic variations and for other applications.

In the traditional method, the proportion of positive clones is often low and is mainly dependent on the skill of the operator. An inexperienced operator may have difficulty obtaining amplification fragments, or most of the clones might not contain SSRs. The integration of the magnetic bead-based FIASCO method in the MFCM-Chip for SSR marker isolation could avoid those drawbacks through highly efficient washing and automated controlled manipulation within a short period of time. Compared to the traditional method, the MFCM-Chip-based assay could dramatically reduce reagent consumption and time. This cost-effective platform will facilitate microchip-based FIASCO implementation with a wide variety of materials. We believe that this device could permit the simultaneous isolation of SSR markers from several different materials. Its successful application will increase interest in applying microfluidic chip technology to other molecular selection processes.

Conclusions

In this study, we presented the design, fabrication, and characterization of a high-efficiency SSR marker isolation device using SPMBs and an MFCM-Chip. The conventional FIASCO method, which is conducted in an Eppendorf tube, is laborious, costly, and time consuming and requires multiple rounds of washing. In contrast to the conventional method, the method proposed here is automated, requires lower reagent consumption and less time, and can increase the specificity and sensitivity of the results because of its highly efficient washing step. Our technology provides a practical method for simple and efficient SSR marker isolation using minimal reagent volumes without the need for well-trained personnel, and this cost-effective platform will make the FIASCO technique more accessible for routine use with a wide variety of materials.

Acknowledgements

This work was supported by the NSFC (Nos. 31171186, 21175100), the 863 program (2013AA032204), the Hubei Province Natural Science Fund, and the Program for New Century Excellent Talents in University (NCET-10-0656).

Notes and references

[a] State Key Laboratory of Hybrid Rice, College of Life Sciences, Key Laboratory of Analytical Chemistry for Biology and Medicine (Ministry of Education), College of Chemistry and Molecular Sciences, and State Key Laboratory of Virology, Wuhan University, Wuhan 430072, PR China. E-mails: ljli@whu.edu.cn (Lijia Li), zlzhang@whu.edu.cn (Zhi-Ling Zhang); Tel/faxs: +86-27-68754505 (Lijia Li), +86-27-68754067 (Zhi-Ling Zhang)
[b] State Key Laboratory of Cotton Biology, College of Life Sciences, Henan University, Kaifeng 475004, PR China
† Electronic Supplementary Information (ESI) available: Further experimental methods and results information. See DOI:10.1039/b000000x/
[1] These authors contributed equally to this work.

1. C. Schlötterer, *Nat Rev Genet*, 2004, **5**, 63-69.
2. M. Koopman, S. Venderbosch, I. D. Nagtegaal, J. H. van Krieken and C. J. Punt, *Eur J Cancer*, 2009, **45**, 1935-1949.
3. A. Mentink, M. Hulsman, N. Groen, R. Licht, K. J. Dechering, J. van der Stok, H. A. Alves, W. J. Dhert, E. P. van Someren, M. J. Reinders, C. A. van Blitterswijk and J. de Boer, *Biomaterials*, 2013, **34**, 4592-4601.
4. M. Ashraf and M. R. Foolad, *Plant Breeding*, 2013, **132**, 10-20.
5. A. G. Griffiths, B. A. Barrett, D. Simon, A. K. Khan, P. Bickerstaff, C. B. Anderson, B. K. Franzmayr, K. R. Hancock and C. S. Jones, *BMC Genomics*, 2013, **14**, 388-405.
6. R. K. Kalia, M. K. Rai, S. Kalia, R. Singh and A. K. Dhawan, *Euphytica*, 2011, **177**, 309-334.
7. L. Zane, L. Bargelloni and T. Patarnello, *Mol Ecol*, 2002, **11**, 1-16.
8. D. Mark, S. Haeberle, G. Roth, F. von Stetten and R. Zengerle, *Chem Soc Rev*, 2010, **39**, 1153-1182.
9. S. Haeberle, D. Mark, F. v. Stetten and R. Zengerle, in *Microsystems and Nanotechnology*, Springer, 2012, pp. 853-895.
10. P. Liu, R. J. Meagher, Y. K. Light, S. Yilmaz, R. Chakraborty, A. P. Arkin, T. C. Hazen and A. K. Singh, *Lab Chip*, 2011, **11**, 2673-2679.
11. T. Geng, N. Bao, M. D. Litt, T. G. Glaros, L. Li and C. Lu, *Lab Chip*, 2011, **11**, 2842-2848.
12. M. Cho, Y. Xiao, J. Nie, R. Stewart, A. T. Csordas, S. S. Oh, J. A. Thomson and H. T. Soh, *Proc Natl Acad Sci U S A*, 2010, **107**, 15373-15378.
13. K. Sato, K. Mawatari and T. Kitamori, *Lab Chip*, 2008, **8**, 1992-1998.
14. M. A. M. Gijs, F. Lacharme, and U. Lehmann, *Chem Rev*, 2010, **110**, 1518–1563.
15. H. C.Tekin and M. A. M. Gijs, *Lab Chip*, 2013, **13**, 4711-4739.
16. M. A. Hayes, T. N. Polson, A. N. Phayre and A. A. Garcia, *Anal Chem*, 2001, **73**, 5896-5902.
17. F. Lacharme, C, Vandevyver, M. A. M. Gijs, *Anal Chem,* 2008, **80**, 2905-2910.
18. S. Bronzeau and N. Pamme, *Anal Chim Acta*, 2008, **609**, 105–112.
19. M. Slovakova, N. Minc, Z. Bilkova, C. Smadja, W. Faigle, C. Fütterer, M. Taverna, and J.L. Viovy, *Lab Chip*, 2005, **5**, 935-942.
20. X. Yu, X. Feng, J. Hu, Z. L. Zhang and D. W. Pang, *Langmuir*, 2011,**27**, 5147-5156.
21. X. Yu, H. S. Xia, Z. D. Sun, Y. Lin, K. Wang, J. Yu, H. Tang, D. W. Pang and Z. L. Zhang, *Biosens Bioelectron*, 2013, **41**, 129-136.
22. M. Vaculovicova, K. Smerkova, J. Sedlacek, J. Vyslouzil, J. Hubalek, R. Kizek and V. Adam, *Electrophoresis*, 2013, **34**, 1548-1554.
23. R. Wilson, *Nucleic Acid Ther*, 2011, **21**, 437-440.
24. R. J. S. Derks, A. Dietzel, R. Wimberger-Friedl and M. W. J. Prins, *Microfluid Nanofluid*, 2007, **3**, 141-149.
25. J. D. Adams, U. Kim and H. T. Soh, *Proc Natl Acad Sci U S A*, 2008, **105**, 18165-18170.
26. A. Csordas, A. E. Gerdon, J. D. Adams, J. R. Qian, S. S. Oh, Y. Xiao and H. T. Soh, *Angew Chem Int Ed*, 2010, **49**, 355-358.
27. X. H. Lou, J. R. Qian, Y. Xiao, L. Viel, A. E. Gerdon, E. T. Lagally, P. Atzberger, T. M. Tarasow, A. J. Heeger and H. T. Soh, *Proc Natl Acad Sci U S A*, 2009, **106**, 2989-2994.

